1. Title: Calcitonin Gene-Related Peptide (CGRP) Receptor Antagonism Reduces Motion Sickness Indicators in Mouse Models of Vestibular Migraine.

2. Authors: Shafaqat M. Rahman[1] & Anne E. Luebke[2*]

[1]Department of Biomedical Engineering

University of Rochester

Rochester NY 14627

[2]Departments of Biomedical Engineering and Neuroscience

University of Rochester Medical Center

Rochester, NY 14642

aluebke@ur.rochester.edu

(*address for correspondence) aluebke@ur.rochester.edu

3. Abstract:

Migraine and vestibular migraine (VM) are associated with enhanced motion sensitivity, and VM is the most common cause of spontaneous vertigo but remains poorly understood. It is now accepted that migraine involves the neuropeptide Calcitonin Gene-Related Peptide (CGRP); yet, it is not clear if CGRP signaling or it's antagonism is involved in motion sensitivity of VM symptoms. Recent murine models of migraine used injections of CGRP or other migraine triggers (sodium nitroprusside (SNP) to induce migraine sensitivities, yet it is not known if these triggers can induce VM sensitivities. Moreover, it is not known if migraine blockers used in preclinical migraine models, can also block the motion-sensitivity of VM. To better understand CGRP's role in VM motion sensitivity, we investigated two measures of motion sickness assessment (MSI scoring and motion-induced thermoregulation) after systemic injections of either CGRP or SNP in the wildtype C57B6/J mice, and found that MSI measures were confounded by CGRP's effect on based on gastric distress, yet assessing motion sensitivity using thermoregulation was robust for both migraine triggers, and CGRP receptor antagonism by olcegepant, but not triptan treatments, rescued CGRP's effect on increased motion sensitivity.

4. Sections:

Introduction: Migraine and vestibular migraine (VM) are associated with enhanced motion sickness, and VM is the most common cause of spontaneous vertigo but remains poorly understood (1-3). VM patients exhibit lower motion perception thresholds compared to healthy controls but no difference in vestibulo-ocular (VOR) thresholds; VM patients also showed enhanced susceptibility to motion sickness both during and after rotation (3). Interestingly, Wang and Lewis (2016) found that in VM patients, but not in migraine or healthy controls, the residual sensory conflict between gravitational (otolith) and rotational (semicircular canal) cues were correlated with motion sickness susceptibility, suggesting otolith/canal misintegration in VM (4).

The diagnostic criteria for human motion sickness have recently been updated (5) and are included in the international classification of vestibular disorders. The major symptoms of motion sickness include facial pallor, nausea, vomiting, gastric awareness and discomfort, sweating, and hypothermia. Motion sickness-induced hypothermia is broadly expressed phylogenetically in humans, mice, rats, and musk shrews. (6, 7). However, rodent models of motion sickness have been constrained because rodents do not vomit and pica eating behavior is thought to be an alternative to vomiting, yet pica has not been shown to be a sensitive measure of motion sickness (8). Instead, piloerection, tremor, fecal and urinal incontinence have been used in scoring criteria called the motion sickness index (MSI) to quantify the degree of motion sickness-like behavior experienced by rats and mice to emetic stimuli (8, 9). In comparison, thermoregulatory changes can be used to assess motion sickness, which in the mouse model involves a decrease in head temperature (hypothermia) and a transient tail-skin vasodilation early in the onset of provocative motion (7). In further detail, tail vasodilations to provocative motion have been reported to precede events of etching and vomiting in the musk shrew, serving as a potential index for motion-induced nausea in experimental rodent models.

Despite the high prevalence of VM, the underlying mechanisms have yet to be defined. It is now accepted that migraine involves the neuropeptide Calcitonin Gene-Related Peptide (CGRP) (10-14). CGRP is upregulated during migraine attacks (15, 16), infusion of CGRP can induce migraine (16), and

antibodies that block CGRP or its receptor can effectively treat most migraines (17, 18); yet, it is not clear that CGRP signaling antagonism is involved in VM symptoms.

Recent animal models of migraine use injections of CGRP or other migraine triggers - such as sodium nitroprusside (SNP) which generates nitric oxide and can stimulate CGRP release – to induce allodynic responses to touch (14, 19) and light-aversive behavior ((20, 21). However, it is not known if these triggers can induce VM symptoms in preclinical models. Moreover, it is not known if migraine blockers used in preclinical models of light sensitivity and allodynia of migraine can also block the motion sensitivity of VM.

To better understand CGRP's role in VM motion-sickness susceptibility, we investigated two measures of motion sickness assessment (MSI scoring and motion-induced thermoregulation) after systemic injections of either CGRP or SNP in the wildtype C57B6/J mouse. In this study, we found that MSI measures based on gastric distress were lessened by CGRP antagonism, yet this was driven by CGRP's effect solely on the gastric system which was not observed with SNP. However, the motion-induced thermoregulation model was robust and CGRP receptor antagonism by olcegepant, but not triptan treatments, relieved CGRP's effect on increased motion sickness susceptibility in VM. Our studies provide a strong premise that antagonizing CGRP signaling will be effective for treating VM, as it has been shown to be highly effective for typical migraine.

Results:

CGRP and SNP's effects on motion sickness index

We studied the effects of CGRP release (n = 9M/10F) on motion sickness indicators and whether the CGRP receptor antagonist olcegepant or the $5HT_{1D}$ receptor agonist sumatriptan could mitigate the occurrence of these indicators. Motion sickness index (MSI) was computed by a summation of criteria depicted in **Fig. 1A**, and this summation was recorded at three different time points - pre-injection, post-injection, and after the vestibular challenge (VC) – for each treatment. Mixed-effects statistical models were used to assess differences in MSI outcomes across two factors: time of criteria measurement and treatment **(Table 1).** While no effect of sex was seen on motion sickness indicators, an increasing trend

of MSI outcomes was observed after injection of treatment and after the VC **(Fig. 1B, C, and D).** Significant differences were seen when comparing time of criteria measurements as described: pre-injection versus post-VC ($F = 846.7$, $p < 0.0001$), post-injection vs post-VC ($F = 904.1$, $p < 0.0001$), and pre-injection versus post-injection ($F = 74.7$, $p < 0.0001$) **(Table 1).** Tukey post hoc analysis compared MSI outcomes between treatments after the vestibular challenge, and significant increases in MSI were seen after delivery of 1x CGRP (adj. $p < 0.0001$) or 1x CGRP + 1x sumatriptan (adj. $p = 0.0002$) compared to vehicle control. No difference in MSI was seen between vehicle and 1x CGRP + 1x olcegepant (adj. $p = 0.98$). A similar observation of increasing MSI outcome was seen with IP SNP administration at subsequent time points **(Fig. 1E, F, and G)**. For SNP treated animals (n = 9M/9F), significant differences were seen in MSI outcomes when comparing pre-injection vs post-VC ($F = 267.8$, $p < 0.0001$), post-injection vs post-VC ($F = 136.6$, $p < 0.0001$) and pre-injection versus post-injection ($F = 105.6$, $p < 0.0001$). However, Tukey post hoc showed no differences between vehicle and IP SNP groups at each time point unlike what was seen with CGRP **(Table 1).**

Fig. 1

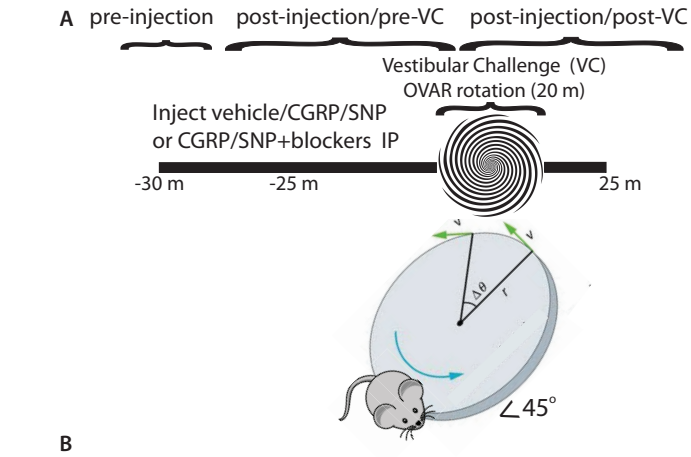

Criterion	*MS Index scoring*
Fecal Granules	0-none; 1 per fecal granule
Piloerection	0-none; 0.6 light; 1.2 severe
Urination	0-none; 1.2 urination
Tremor	0-none; 1.2 tremor

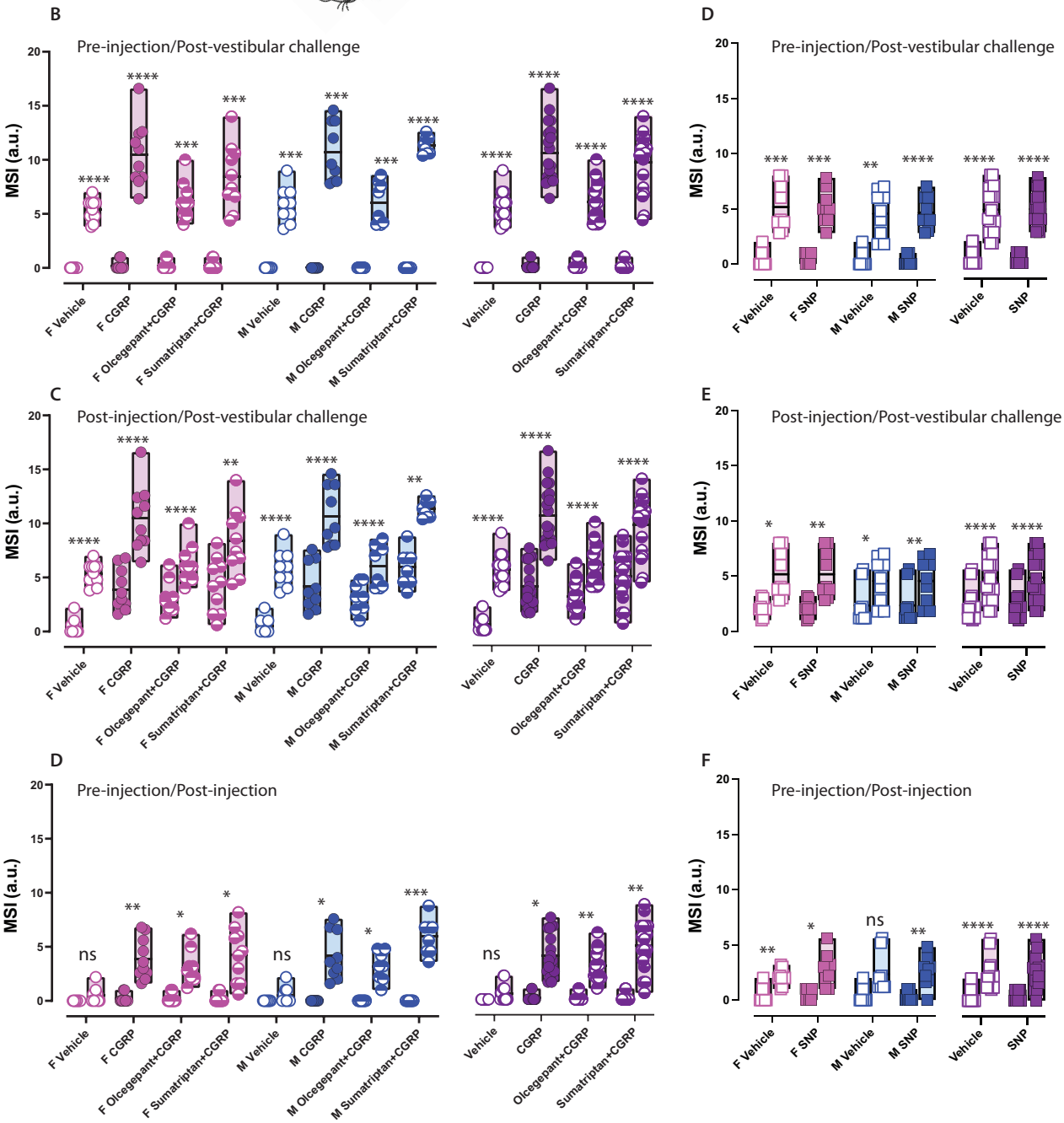

Table 1

CGRP vs CGRP + Blockers				
Analysis	**Factors**	**P value**	**F (DF_n, DF_d)**	**Comparison**
MSI	pre-injection vs post-VC	<0.0001	F (1.0, 18.0) = 846.7	vehicle
				CGRP
	vehicle vs CGRP or CGRP+blockers	<0.0001	F (2.6, 46.1) = 23.2	CGRP + Olcegepant
				CGRP + Sumatriptan
	post-Injection vs post-VC	<0.0001	F (1.0, 18.0) = 904.1	vehicle
				CGRP
	vehicle vs CGRP or CGRP+blockers	<0.0001	F (2.4, 43.6) = 24.7	CGRP + Olcegepant
				CGRP + Sumatriptan
	pre-injection vs post-Injection	<0.0001	F (1., 18.0) = 74.7	vehicle
				CGRP
	vehicle vs CGRP or CGRP+blockers	0.0006	F (2.8, 50.0) = 7.1	CGRP + Olcegepant
				CGRP + Sumatriptan
Feces	pre-injection vs post-VC	<0.0001	F (1.0, 18.0) = 469.2	vehicle
				CGRP
	vehicle vs CGRP or CGRP+blockers	<0.0001	F (2.6, 45.9) = 24.9	CGRP + Olcegepant
				CGRP + Sumatriptan
	post-Injection vs post-VC	<0.0001	F (1.0, 18.0) = 303.4	vehicle
				CGRP
	vehicle vs CGRP or CGRP+blockers	<0.0001	F (2.3, 41.2) = 26.8	CGRP + Olcegepant
				CGRP + Sumatriptan
	pre-injection vs post-Injection	<0.0001	F (1.0, 18.0) = 205.6	vehicle
				CGRP
	vehicle vs CGRP or CGRP+blockers	<0.0001	F (2.1, 37.4) = 21.8	CGRP + Olcegepant
				CGRP + Sumatriptan
SNP				
Analysis	**Factors**	**P value**	**F (DFn, DFd)**	**Comparison**
MSI	pre-injection vs post-VC	<0.0001	F (1.0, 17.0) = 267.8	vehicle
	vehicle vs SNP	0.8863	F (1.0, 17.0) = 0.02	SNP
	post-Injection vs post-VC	<0.0001	F (1.0, 17.0) = 136.6	vehicle
	vehicle vs SNP	0.5738	F (1.0, 17.0) = 0.3	SNP
	pre-injection vs post-Injection	<0.0001	F (1.0, 17.0) = 105.6	vehicle
	vehicle vs SNP	0.338	F (1.0, 17.0) = 1.0	SNP
Feces	pre-injection vs post-VC	<0.0001	F (1.0, 17.0) = 44.3	vehicle
	vehicle vs SNP	0.7702	F (1.0, 17.0) = 0.1	SNP
	post-Injection vs post-VC	0.0029	F (1.0, 17.0) = 12.1	vehicle)
	vehicle vs SNP	0.7524	F (1.0, 17.0) = 0.1	SNP
	pre-injection vs post-Injection	<0.0001	F (1.0, 17.0) = 33.1	vehicle
	vehicle vs SNP	0.3159	F (1.0, 17.0) = 1.1	SNP

Motion sickness outcome is driven by feces criteria

A closer observation of MSI outcomes showed that the main driver of MSI is the magnitude of feces collected. Across the three different time points, differences in collected feces were significant and mimicked MSI outcomes for both IP CGRP and IP SNP **(Fig. 2A, B, and C).** Mixed-effects analyses were used to assess differences in feces collected (**Table 1**), and Tukey post-hoc analyses after the vestibular challenge showed increased fecal excretion after 1x CGRP (adj. $p < 0.0001$) and after 1x CGRP + 1x sumatriptan (adj. $p = 0.0001$). In contrast, mice treated with 1x CGRP + 1x olcegepant showed no significant difference in excreted feces compared to vehicle control (adj p. = 0.97). During the test, we observed that mice treated with 1x CGRP or 1x CGRP + 1x sumatriptan exhibited diarrhea while mice treated with 1x CGRP + 1x olcegepant did not. Mice treated with 1x SNP did not exhibit diarrhea across all time points, and no differences were observed in collected feces across treatment **(Fig. 2D, E, and F**). PUT outcomes were also shown across time points and treatments. PUT is calculated by summing observed piloerection, urination, and tremor during the study. While PUT outcomes increased with every timepoint like MSI and observed feces, no differences were seen between treatments (**Fig. 3**). These results suggest that a flaw in the motion sickness assay corresponds to its exaggerated emphasis on fecal excretion.

Fig. 2

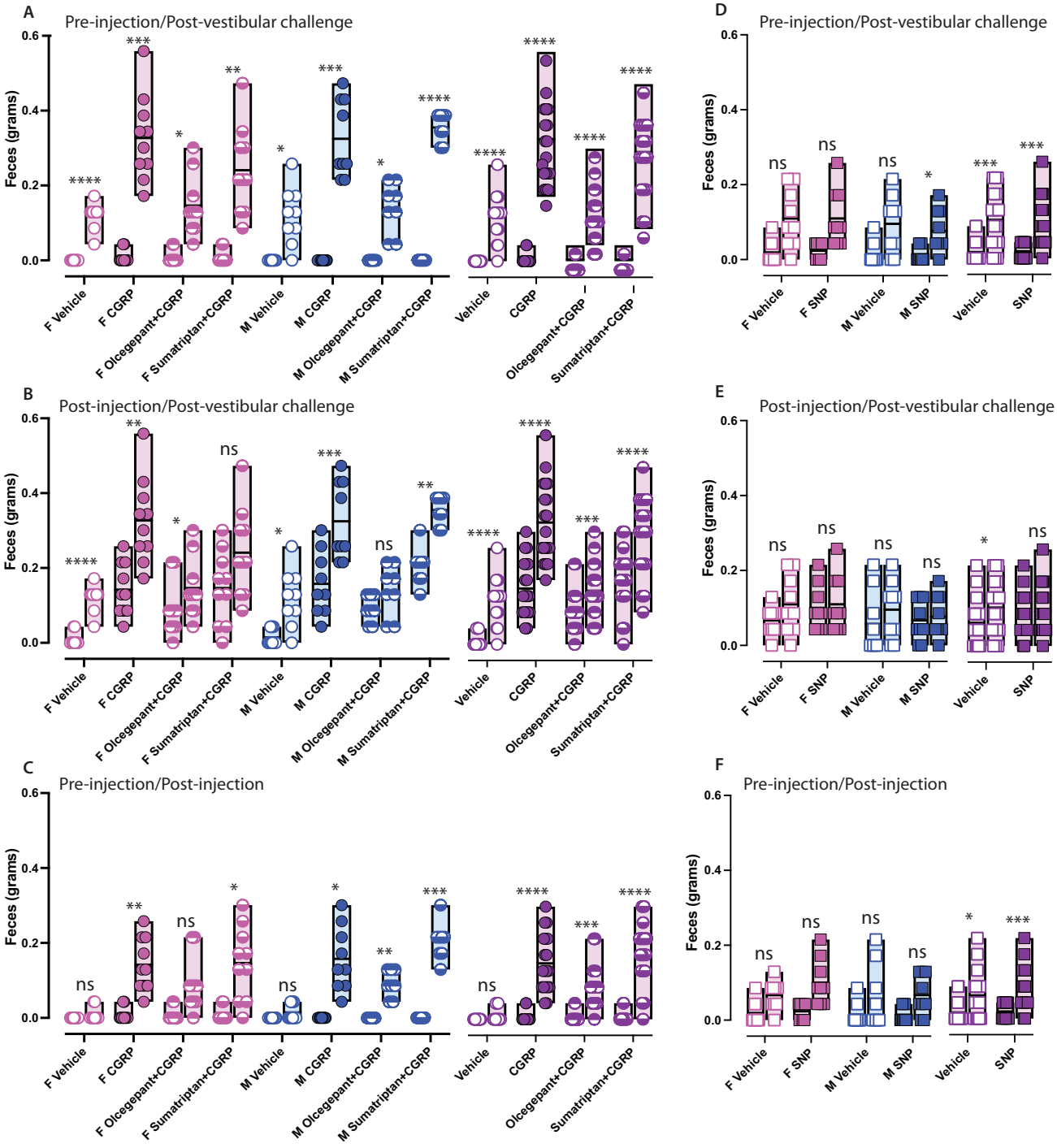

Fig. 3

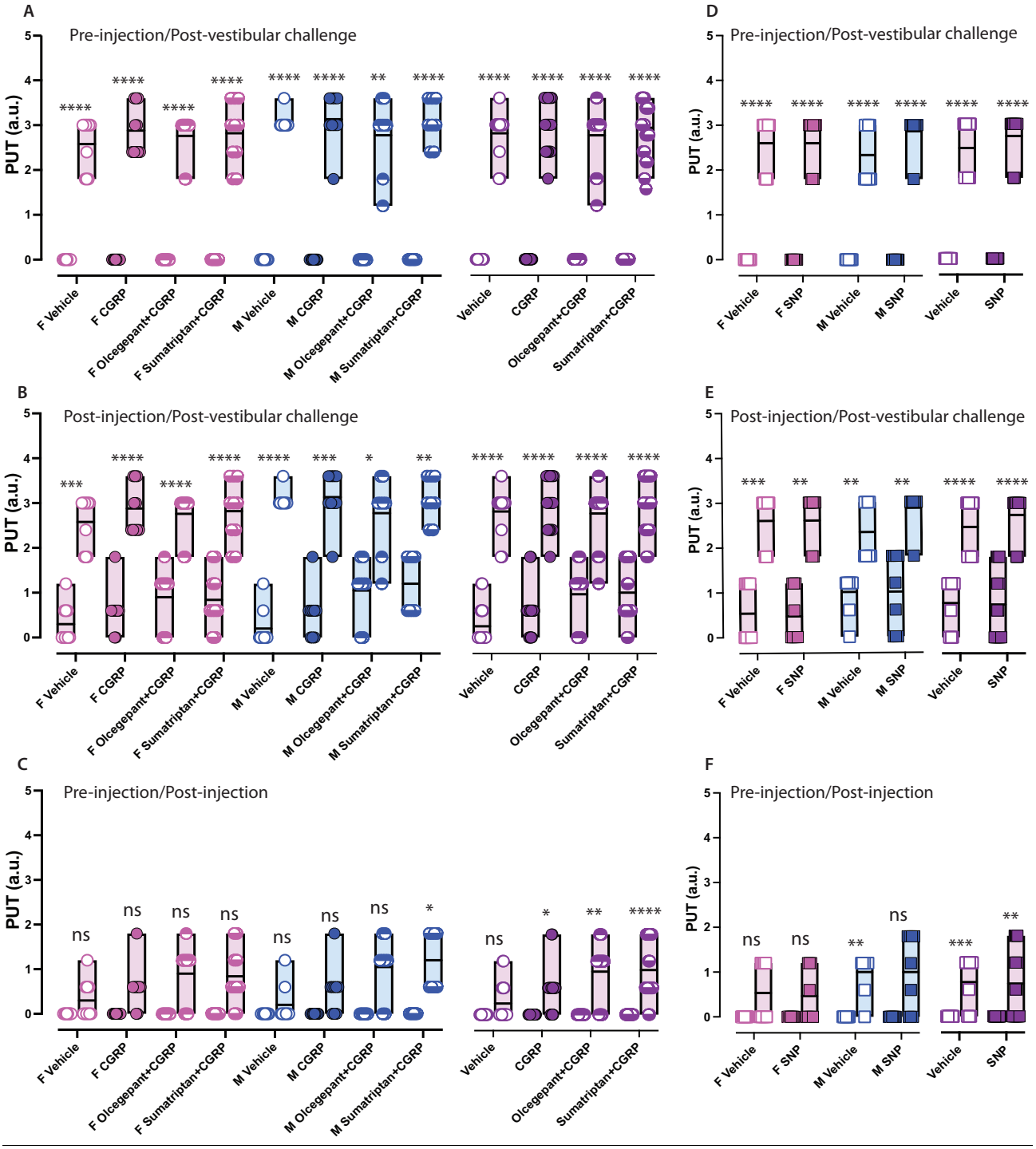

Hypothermia and tail vasodilations occur during provocative motion and not stationary testing

Motion-induced thermoregulation in mice was assessed by measuring hypothermia and tail vasodilations to provocative motion. The provocative motion involved an orbital rotation (1 cm orbital displacement) at 75 rpm (**Fig. 4A**). After a five-minute baseline recording, mice (n = 32M/25F) are challenged with provocative motion (t = 0 mins, rotation = ON) and exhibited gradual hypothermia until the end of the motion (t = 20 mins, rotation = OFF). 2nd order curve fits calculated the *delta head drops* – an estimate of the mouse's experienced hypothermia – to be -1.22^{o}C for females and -1.62 ^{o}C for males with R^2 fits equal 0.9 for both curves (**Fig. 4B).** In addition to the hypothermia, mice exhibited transient but significant increases in tail temperature during the first 10 minutes of the provocative motion. The tail temperature increase was quantified and labeled as the *delta tail vasodilation* and is computed by subtracting the tail temperature at time t = 0 from the max tail temperature measured during the first 10 minutes of the rotation ($0 \leq t \leq 10$). During provocative motion testing after treatment of vehicle control, delta tail vasodilations were observed in females (4.6 ± 0.3 ^{o}C) and males (6.1 ± 0.4 ^{o}C) (**Fig. 4D**). To ensure that the hypothermia and the tail vasodilations were physiological responses to the provocative motion stimulus, a separate group of mice (n = 9F/10M) was tested similarly but for stationary testing. No observed hypothermia or transient vasodilations were seen in mice of either sex during the stationary tests (**Fig. 4C** and **E**).

Fig. 4

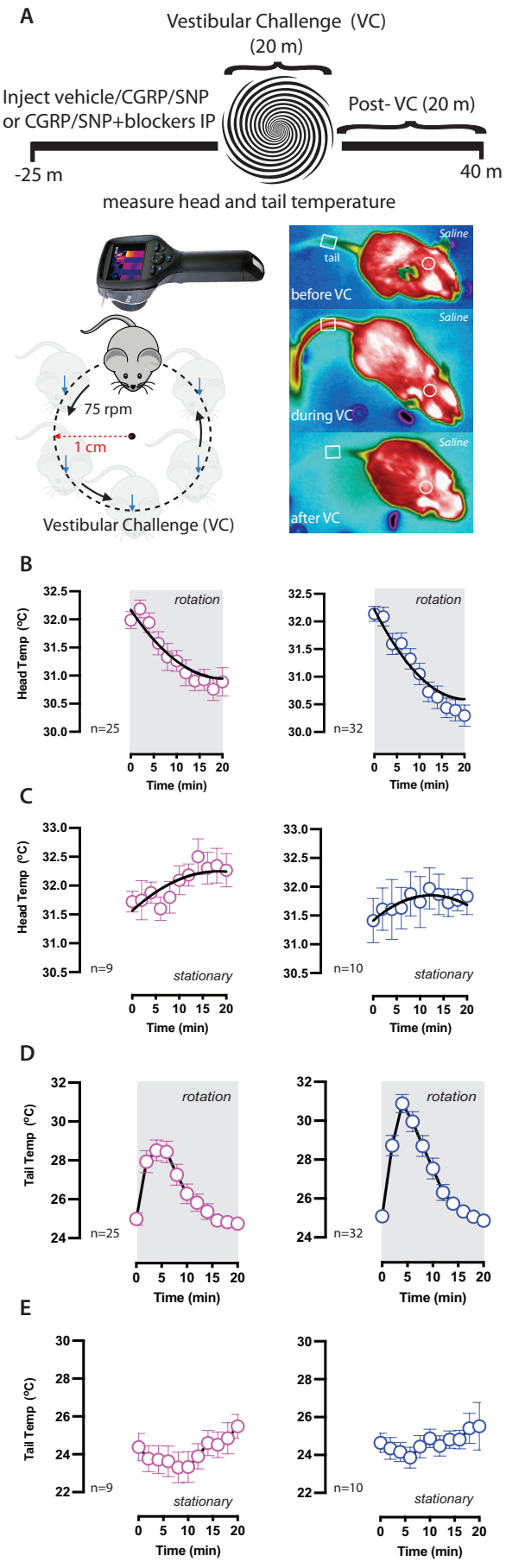

CGRP and SNP's effects during stationary test

To exclude the possibility of thermoregulatory changes that may be due to the treatments - CGRP and SNP - and not the rotation, a secondary stationary test was done on mice (n = 9M/9F) who were tested with 1x CGRP and 1x SNP. These mice were measured, without rotation, for 20 minutes. No differences were seen in the head or tail temperatures after 1x CGRP or 1x SNP testing compared to vehicle control, and hypothermia or increased tail temperatures were not observed (**Fig. 5A, B, D, E).**

Test-retest reliability during provocative motion

Mice were assessed for test-retest reliability of hypothermia to provocative motion and this was done 4 to 7 days apart (n = 9M/8F). Under vehicle control, male and female mice exhibited hypothermia during the provocative rotation and this response was repeatably observed in the retest. In **Fig. 5C**, 2nd order curve fits were generated for test-retest head curves and strong fits were seen for female (Pearson's *r (23)* = 0.87, $p < 0.0001$) and for male (Pearson's *r (23)* = 0.89, $p< 0.0001$). Delta head drops are calculated as an estimate of the magnitude of hypothermia, and similar estimates were seen for females (mean head drop $_{test}$: -1.2 ^{o}C, mean head drop $_{retest:}$ -1.2 ^{o}C) and in males (mean head drop $_{test}$: -1.3 ^{o}C, mean head drop $_{retest: -}$1.2 ^{o}C). In addition, in figure **5F**, similar tail temperature profiles were observed during test-retest for females (Pearson's *r* (23) = 0.92, $p < 0.0001$) and for male (Pearson's *r (23)* = 0.95, $p < 0.001$). Delta tail vasodilations were observed to be similar in magnitude for females (mean vasodilation $_{test}$: 4.0 ± 0.8 ^{o}C, mean vasodilation $_{retest}$: 4.2 ± 0.8 ^{o}C) and for males (mean vasodilation $_{test}$: 4.9 ± 0.8 ^{o}C, mean vasodilation $_{retest}$: 4.9 ± 0.9 ^{o}C).

Fig. 5

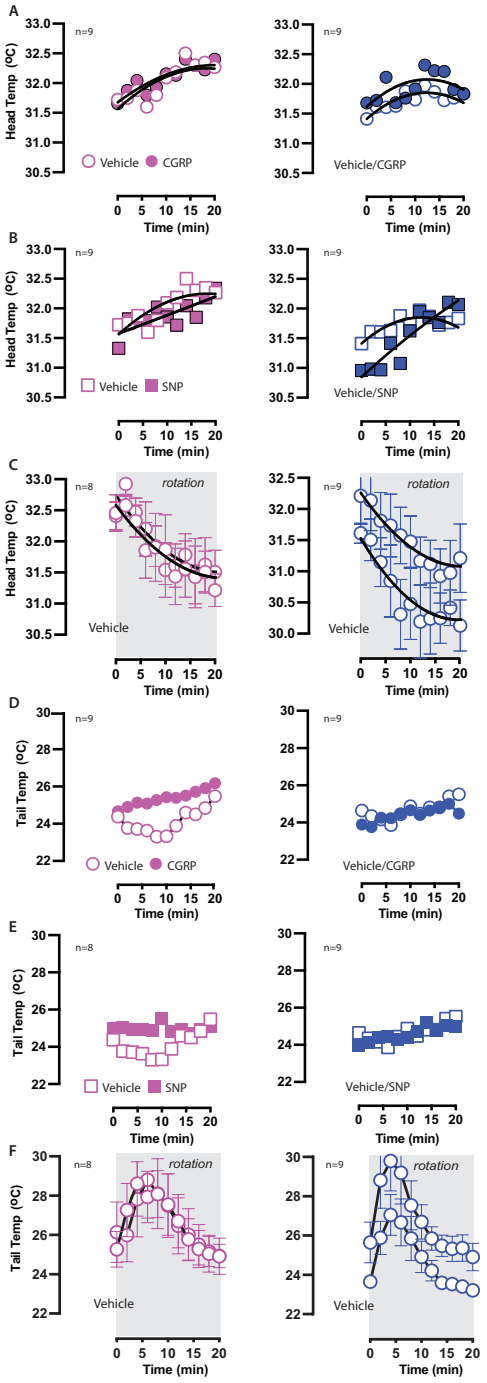

CGRP and SNP affect motion-induced thermoregulation in C57/B6J mice

Mice were tested after IP 1x CGRP administration (n = 20M/18F). 2nd order curve fits were used to compute the recovery of head temperatures back to baseline values after the hypothermia and to compute delta head drops. In the cohort of mice used for assessing CGRP's effects, mice of either sex experienced extended recovery times after 1x CGRP (female: 28.4 mins, R^2 = 0.73; male: 25.4 mins, R^2 = 0.83) compared to their vehicle control (female: 20.3 mins, R^2 = 0.86; male: 20.4 mins, R^2 = 0.85), suggesting that 1x CGRP may impact a mouse's ability to recover from the provocative motion (**Fig. 6A and B**). We saw no differences in delta head drops between vehicle and CGRP for either sex. **Fig. 6E and F** show tail temperature profiles after 1x CGRP and delta tail vasodilations were also computed. 100% of mice exhibited normal delta tail vasodilations after vehicle control administration but a majority of mice (83.3% female, 45% male) exhibited diminished delta tail vasodilations (< 1.5^{o}C) after 1x CGRP administration. Due to the diminished delta vasodilations and the extended recovery times detected after CGRP testing, it is assumed that 1x CGRP impacted a mouse's natural response to the provocative motion and impacted their nausea response. In parallel, a different group of mice (n = 8M/8F) was used to assess SNP's effects on motion-induced thermoregulation, and temperature profiles were analyzed similarly. When measuring head temperatures, we did not observe any differences in recovery time back to baseline or in delta head drops (**Fig. 6C and D**). However, similar to CGRP, 1x SNP impacted delta tail vasodilations. After vehicle control, 100% of mice showed observable, normal delta tail vasodilations assumed for this behavior but a majority of mice in this testing cohort (100% females, 75% males) exhibited diminished vasodilations after 1x SNP similarly to what was seen with 1x CGRP (**Fig. 6G and H**).

Dose-dependent response of CGRP or SNP on tail vasodilations

While 1x concentrations were used for the motion sickness assay in this study and these concentrations are based on previous studies looking at CGRP or SNP effects on cutaneous allodynia in similar mouse models, it was unclear whether these doses were required to elicit thermoregulatory changes in mice or if lower doses would suffice. To answer this question, a dose-dependent response curve was tested in mice (n = 9M/9F) and delta tail vasodilations were analyzed at 0.1x, 0.5x, and 1x

concentrations of IP CGRP or IP SNP (**Fig. 6I, J, and L**). In the CGRP group (n = 10M/9F), 0.1x CGRP had no significant effects on delta tail vasodilations in either sex. However, significant differences were observed when comparing delta tail vasodilations between vehicle and 0.5x CGRP in females ($p < 0.0002$) and in males ($p < 0.02$). Significant differences in delta tail vasodilations were also seen when comparing vehicle and 1x CGRP in both sexes ($p < 0.0001$). When assessing SNP's effects (n = 8F/8M), no significant differences were seen at 0.1x and 0.5x SNP compared to vehicle control, but a significant difference was seen when comparing vehicle to 1x SNP in females ($p < 0.02$) and in males ($p < 0.0002$). The greatest effect of CGRP and SNP on delta tail vasodilations was observed at their 1x concentration and these concentrations were used to assess the blockers olcegepant and sumatriptan.

Fig. 6

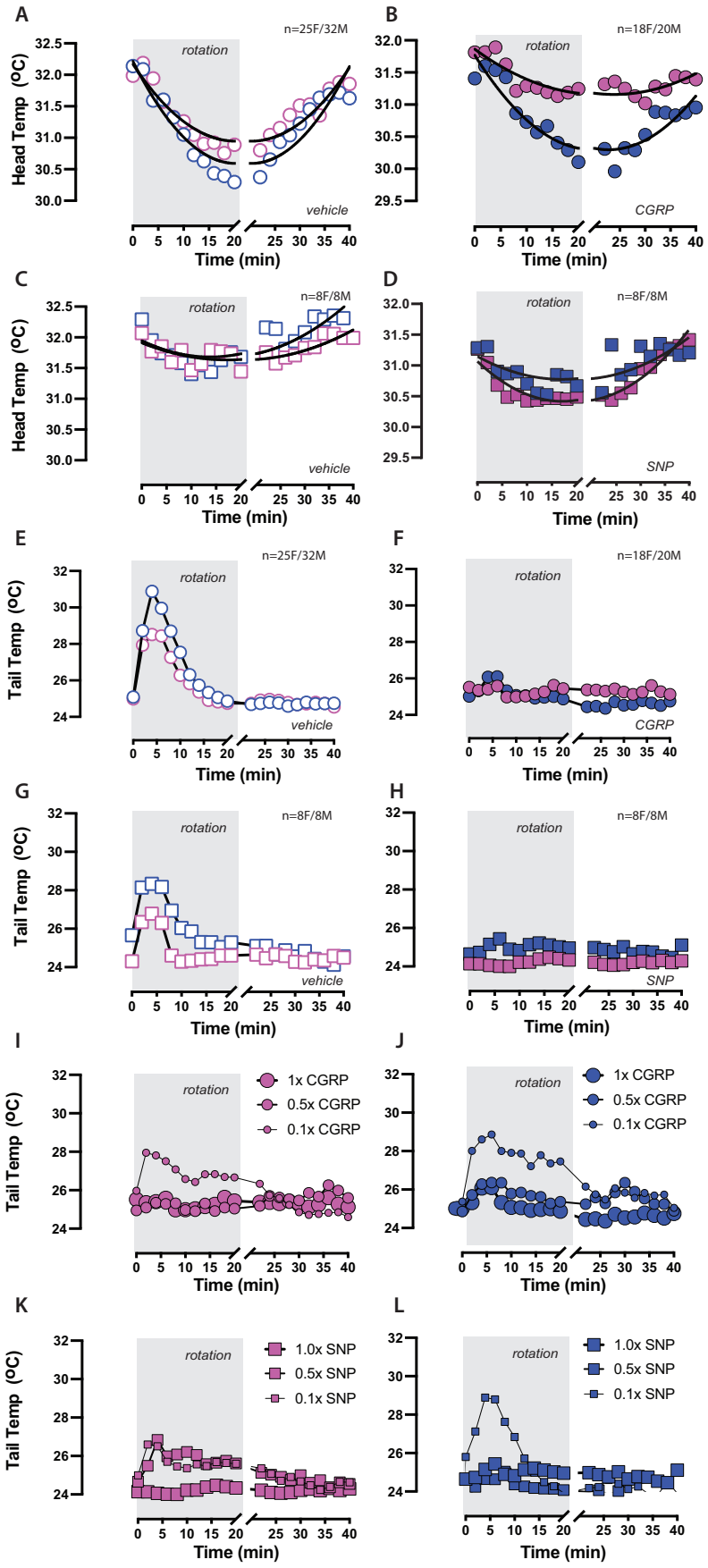

Olcegepant but not triptans protect against CGRP's effects on tail vasodilations

While we saw no differences in delta head drops between vehicle and CGRP testing, administration of 1x CGRP diminished the delta tail vasodilations in nearly all mice and altered their nausea response, and so it was hypothesized that mice would regain their tail vasodilation with further treatment of CGRP+olcegepant or CGRP+sumatriptan. To conduct adequate comparisons between the differences seen with CGRP or CGRP + blockers, mice were excluded that did not experience delta tail vasodilations greater than or equal to +1.5^{o}C during vehicle control, and these mice were not further tested with IP CGRP/SNP or IP CGRP/SNP +blockers. Of the total mice tested for 1x CGRP testing for motion-induced nausea, eligible, healthy mice were randomized to assess for 1x CGRP + 1x olcegepant (n = 10M/7F) or 1x CGRP + 1x sumatriptan (n = 10M/8F) but were not tested for both. In addition, these mice were tested for motion-induced nausea after IP delivery of only 1x olcegepant (n = 7F/10M) or only 1x sumatriptan (n = 6F/10M), and no differences were seen in delta tail vasodilations when compared to their vehicle control (not shown). In both male and female mice, tail temperature profiles were observed for vehicle, 1x CGRP, 1x CGRP + 1x olcegepant, and 1x CGRP + 1x sumatriptan, and delta tail vasodilations were analyzed (**Fig. 7A, B, C, D, E, F, G, and H**). Before-after plots are used to show within-subject changes in delta tail vasodilations in animals tested with either olcegepant or sumatriptan and a floating bar plot is used to compare all animals for assessing CGRP's effects on delta tail vasodilations (**Fig. 7I, J and M**). Mixed-effects analysis on delta tail vasodilations showed that the factors CGRP/CGRP+Blockers ($F = 58.7$, $p < 0.0001$) and sex ($F = 15.4$, $p = 0.0002$) to be significant (**Table 2)**. Tukey post-hoc analysis showed a significant difference between vehicle and CGRP (adj. $p < 0.0001$) and vehicle versus CGRP+sumatriptan (adj. $p<0.001$) for male and female mice, while no significant differences were seen between vehicle vs IP CGRP+olcegepant for either sex. When assessing CGRP+blockers on delta tail vasodilations, some mice (57.1% female, 20% male) still exhibited diminished tail vasodilations after administration of 1x CGRP + 1x olcegepant, but a greater percentage of mice (87.5% female, 60% male) remained impaired after 1x CGRP + 1x sumatriptan. During the dose-dependent response study, while no significant effects were seen with 0.1x CGRP, mice treated with 0.5x CGRP and experienced diminished vasodilations were later tested with 0.5x CGRP + 1x olcegepant. A majority of these mice were rescued, as only 14.2% of females and

20% of males remained impaired after delivery of olcegepant (**Fig. 7K**). These findings show that olcegepant blocked the effects of CGRP and allowed for a majority of mice to exhibit their normal response to the provocative motion that was not seen with co-administered sumatriptan.

To further explore the effects of triptans on delta tail response, the main study was supplemented by taking a different cohort of mice and assessing the effects of rizatriptan on delta tail vasodilation (**Fig. 7L)**. Mice treated with 1x CGRP + 1x rizatriptan (n = 7M/7F) led to diminished tail vasodilations in females (adj. p = 0.01) and in males (adj. p = 0.003) as similarly seen with 1x CGRP + 1x sumatriptan testing. Rizatriptan was not effective in blocking CGRP's effects, as 75% females and 87.5% males were observed to have diminished tail vasodilations. We also observed that mice appeared to exhibit more "grimace" like features after administration of rizatriptan compared to the other blockers, but we did not assess grimace or related behaviors in this study.

Fig. 7

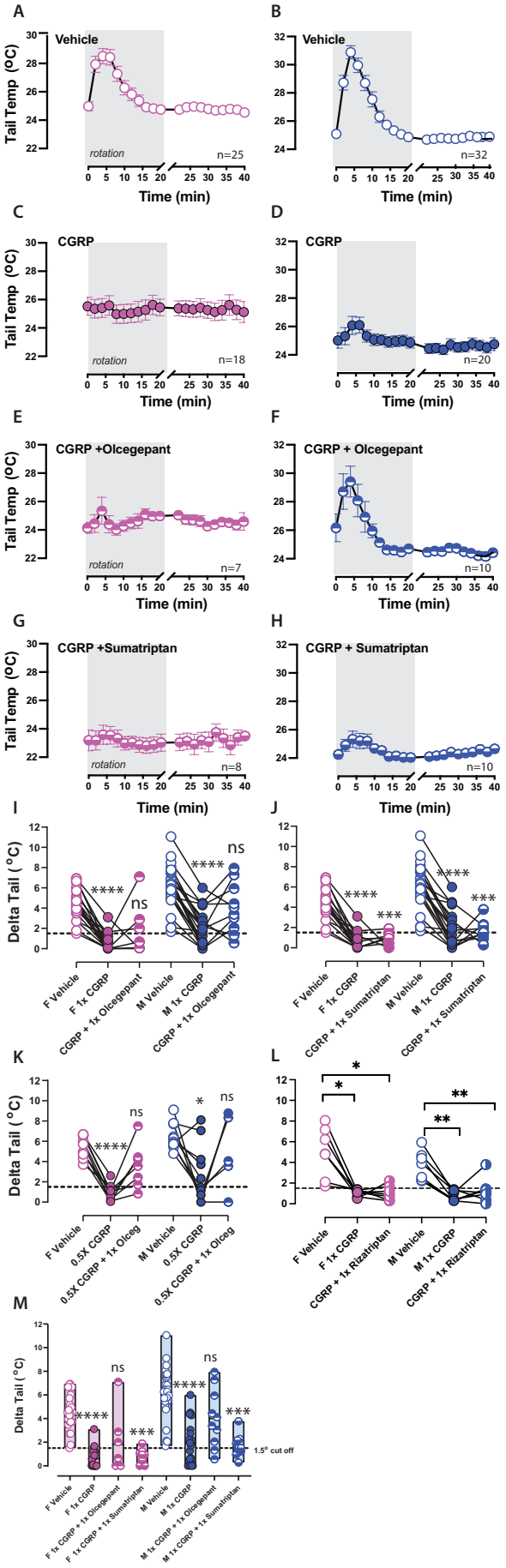

SNP's effects on tail vasodilations are blocked by olcegepant and sumatriptan

Similar to CGRP testing, the effects of the blockers olcegepant and sumatriptan were also assessed against 1x SNP in mice (n = 8M/8F). Due to lower sample sizes compared to CGRP testing, all mice in the SNP group were assessed with olcegepant or sumatriptan. Tail temperature profiles for vehicle control, 1x SNP, 1x SNP + 1x olcegepant, and 1x SNP + 1x sumatriptan were depicted (**Fig. 8A, B, C, D, E, F, G, and H**). Before-after plots were used to show within-subject changes across treatments and a floating bar plot is used to compare all tested animals used for assessing SNP's effects (**Fig. 8I, J and K**). Mixed-effects analyses showed that SNP/SNP+Blockers ($F = 6.0$, $p = 0.003$) to be significant but that sex was not significant ($F = 0.1$, $p = 0.79$). Tukey's post-hoc analysis showed that vehicle vs SNP was significant in male (adj. $p = 0.0002$) and female (adj. $p = 0.015$) mice, but saw no difference between vehicle vs 1x SNP + 1x olcegepant or vehicle vs 1x SNP + 1x sumatriptan (**Table 2**). Blockers were partially effective in mice treated with SNP, as 50% of females and males exhibited reduced tail vasodilations when tested with 1x SNP co-administered with either 1x olcegepant or 1x sumatriptan. We did not further test SNP treated mice with rizatriptan. In summary, **Table 3** is provided to depict the differences in diminished tail vasodilations observed across all treatments (CGRP/SNP + blockers) for male and female mice.

Fig. 8

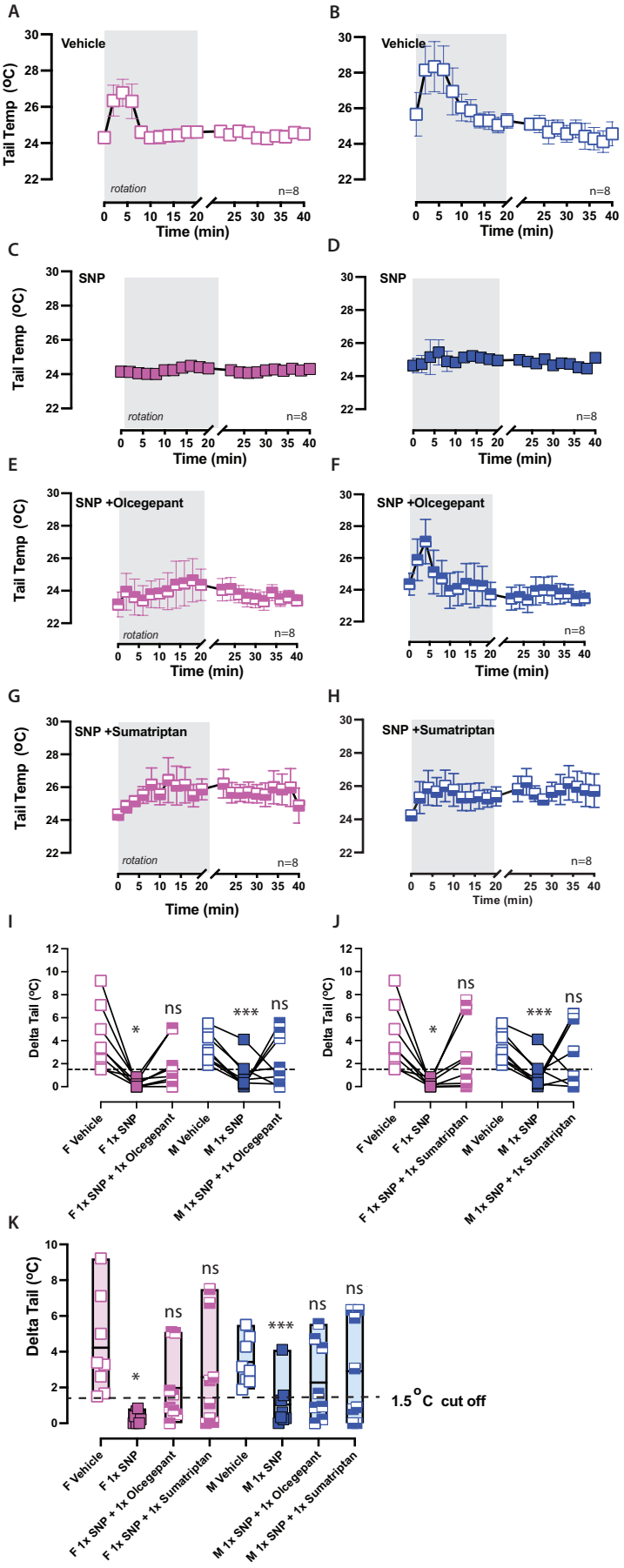

Table 2

Delta Tail - mixed effects models						
Analysis	**Factors**	**P-value**	**F (DFn, DFd)**	**Sex**	**Treatment**	**P-value**
CGRP vs CGRP+Blockers	CGRP/CGRP+Blockers	<0.0001	F (2.0, 45.2) = 58.7	M	vehicle vs. CGRP	<0.001
					vehicle vs. CGRP + olcegepant	0.21
	Sex	0.0002	F (1, 55) = 15.4		vehicle vs. CGRP + sumatriptan	<0.001
				F	vehicle vs. CGRP	<0.001
	CGRP/CGRP Blockers x sex	0.85	F (3, 67) = 0.3		vehicle vs. CGRP + olcegepant	0.1
					vehicle vs. CGRP + sumatriptan	<0.001
SNP vs SNP+Blockers	SNP/SNP+Blockers	0.003	F (2.4, 44.5) = 6.0	M	vehicle vs. SNP	0.0002
					vehicle vs. SNP + olcegepant	0.9131
	Sex	0.79	F (1, 56) = 0.1		vehicle vs. SNP + sumatriptan	>0.9999
				F	vehicle vs. SNP	0.0149
	SNP/SNP+Blockers vs Sex	0.77	F (3, 56) = 0.4		vehicle vs. SNP + olcegepant	0.3741
					vehicle vs. SNP + sumatriptan	0.6164

Table 3

Reduced delta tail vasodilations (< 1.5 °C) during motion-induced thermoregulation		
Treatment	**Female %**	**Males %**
Vehicle	0.0%	0.0%
0.1x CGRP	22.2%	0.0%
0.5x CGRP	77.7%	50.0%
1.0x CGRP	83.3%	45.0%
0.5x CGRP + 1.0x olcegepant	14.2%	20.0%
1.0x CGRP + 1.0x olcegepant	57.1%	20.0%
1.0x CGRP + 1.0x sumatriptan	87.5%	60.0%
1.0x CGRP + 1.0x rizatriptan	75.0%	87.5%
1.0x SNP	100.0%	75.0%
1.0x SNP + 1.0x olcegepant	50.0%	50.0%
1.0x SNP + 1.0x sumatriptan	50.0%	50.0%

Discussion:

In this study, we show that systemic CGRP and SNP injections can induce motion sickness in wildtype C57B6/J mice, and this motion sickness can be antagonized by the CGRP receptor blocker, olcegepant. Interestingly, unlike other migraine symptoms, neither sumatriptan nor rizatriptan were effective in counteracting CGRP's induced motion sickness. We have used two different murine motion sickness assays: 1) MSI and 2) motion-induced thermoregulation. In both assays, provocative motion caused distinct changes, but MSI was too heavily weighted on gastric incontinence to be useful for studying CGRP changes, while the SNP induced migraine model did not cause increased fecal granules but showed no significant differences from vehicle injection. However, the thermoregulation model to provocative motion was robust for both CGRP- and SNP-induced migraine models. Similar rodent studies suggest tail vasodilations are a precursor to emesis and removal of toxins (7). Our data showing CGRP's blunting of tail vasodilations to provocative motion suggests that nausea may be aggravated with CGRP and that olcegepant may be protective but not sumatriptan or rizatriptan. This finding is encouraging, as a study published in March 2020 examined the effects of 2-hour infusion of CGRP in human volunteers on gastrointestinal hyperactivity and nausea, and if sumatriptan can ameliorate these issues. Infusion of CGRP caused gastrointestinal issues and nausea, and pre-treatment of sumatriptan did not ameliorate these symptoms while a CGRP-antagonist was successful (22) and correlates with our preclinical findings. A meta-analysis has also reviewed relevant studies on anti-CGRP treatments for nausea in episode migraine and provides strong support for their use (23). Interestingly, we also observed that female mice were more severely affected by systemic CGRP than their male counterparts, and matches other preclinical studies studying light-aversive behavior and tactile hypersensitivity in mice (24-26).

CGRP signaling and murine motion-sickness indices:

Others have shown in human subjects and in mouse models that CGRP causes diarrhea by disrupting peristaltic intestinal activity and promoting ion and water secretion in the intestinal lumen, and that CGRP signaling antagonism can reverse these effects (27, 28). We have verified that OVAR rotation does further increase gastric distress in mice (increased fecal granules and

diarrhea) and other indices like piloerection and a short-term tremor. Yet, no differences were detected in the occurrence these other symptoms between vehicle, CGRP/SNP, and CGRP/SNP co-administered with blockers (**see Fig. 3**).

However, the motion-induced thermoregulation model revealed differences between vehicle and CGRP/SNP injected mice. Differences in thermoregulatory measures after CGRP-induced motion sickness were blocked by a CGRP receptor antagonist (olcegepant) but not by triptan therapy, while SNP-induced motion sickness was treated by all tested blockers. We also showed that in the absence of provocative motion, there are no thermoregulatory changes as indicated by stationary tests. While male and female mice both showed disrupted thermoregulatory responses to systemic CGRP injections, dose response experiments at 0.05 and 1 mg/kg CGRP show that olcegepant can rescue CGRP-induced nausea in mice, but with limited effectiveness in females at the higher concentration (**Table 3**). This sexual dimorphism is similar to higher incidence of migraine and VM in female patients (29-31) and reports of sexual-dimorphic effects of CGRP both in dura-induced pain, spinal cord neuropathic pain, and preclinical surrogates for allodynia and photophobia in mice (25, 26, 32, 33). To this end, other studies have demonstrated a sex difference in the expression of CGRP receptor components in the trigeminal nucleus (34). Our experiments assessing SNP+blockers on thermoregulation indicate SNP's effects were rescued in some but not all mice - as 50% of females and males responded to olcegepant or sumatriptan - and it is unclear why. NO donors are hypothesized to act on perivascular sensory fibers and central sites to induce CGRP release. Results from studies are mixed, as one study in humans showed sumatriptan to abort headache and allodynia caused by nitroglycerin, and a related study in mice showed olcegepant and sumatriptan to reduce glyceryl trinitrate (GTN)-induced allodynia (35, 36). However, a double blind crossover study provides counter-evidence suggesting olcegepant is ineffective at preventing GTN-induced migraine (37). Additionally, our study's assays aim to assess symptoms of motion sickness and nausea which may require vestibular and emetic signaling pathways distinct from migraine pain and require further exploration in respect to migraine triggers (38, 39). To our understanding, we are the first to use motion-induced

thermoregulation as a preclinical model for vestibular-related issues that may arise in migraine. Future experiments aimed at understanding CGRP's role in other VM symptoms will be required to fully elucidate the role of CGRP-signaling in VM.

Materials & Methods

Animals: C57B6/J mice were obtained from Jackson Laboratories (JAX #664) and were housed under a 12 to 12 day/night cycle under the care of the University Committee on Animal Resources (UCAR) at the University of Rochester. Mice are housed together in cages (max 5 mice per cage) with *ad libitum* access to food, water, and bedding material. Equal numbers of male and female mice were tested and a total of 213 mice (106 M/ 107 F) were used for these studies, and studies were powered sufficiently to detect male/female differences. Prior to all experiments, mice were equilibrated in the testing room controlled for an ambient temperature between 22-23^{o}C for at least 30 minutes, and remained in this room until completion of experiment per testing day. Injections occur after the equilibration period in the testing room. For both motion sickness and motion-induced nausea testing, mice were tested in the range of 2.3 - 6 months of age. This age range in mice correlates to 20-30 years in humans and is within the range of 18 to 44 years that migraine symptoms most likely occur in patients (40). Different cohorts of mice were used to test motion sickness indices and motion-induced nausea. Experimentation occurs from 9:00 am to 4:30 pm during the day cycle to control for behavioral and thermoregulatory changes that may arise from circadian rhythm. For motion-induced nausea testing, mice were screened for instances of patchy fur (alopecia) that could add uncontrolled variance to measured mouse thermoregulation, and thus were not included in this study (41).

Drug administration: Injections were performed intraperitoneally (IP) with a 0.33 x 12.7 insulin syringe. Dulbecco PBS served as the diluent and as the vehicle control. Drugs used to inhibit CGRP-signaling were the CGRP-receptor antagonist olcegepant and the selective serotonin receptor antagonists sumatriptan and rizatriptan. The concentrations are listed: 0.1x, 0.5x, and 1x CGRP were prepared at 0.01, 0.05, and 0.1 mg/kg (rat α-CGRP, Sigma), 1x olcegepant was prepared at 1 mg/kg (BIBN4096, Tocris), 1x sumatriptan was prepared at 0.6 mg/kg (Sigma-Aldrich), 1x rizatriptan was prepared at 0.6 mg/kg (Sigma-Aldrich), and 0.1x, 0.5x, and 1x sodium nitroprusside (SNP)- (Sigma-Aldrich) were prepared at 0.25 mg/kg, 1.25, and 2.5 mg/kg. Injection volumes were calibrated so that each animal

received 1 injection per testing day at ~100 ul. After injection, animals were placed in a separate cage from their home cage to recuperate from injection stress. Mice were tested 20 minutes after delivery of either vehicle, CGRP, CGRP with blockers, or drug controls. Mice were tested 30 minutes after delivery of SNP or SNP with blockers. Animals were gently handled so anesthesia is not needed during injections. Animal procedures were approved by the University of Rochester's Medical Center (URMC) performed in accordance with the standards set by the NIH.

Off-Vertical Axis Rotation (OVAR): The use of OVAR as a vestibular stimulus is evidence based; prior human and rodent studies have used OVAR to test the otolith-ocular reflex and assess semicircular canal-otolith interaction (42-44). Constant velocity OVAR at a tilt can be disorienting and promote motion sickness in human participants (45, 46), and further studies in mice have shown that provocative rotation leads to kaolin consumption – a behavioral marker for illness - and observations of urination, piloerection, and tremor (47). In this study, a two-cage rotator (cage dimensions: 12.7 cm x 8.9 cm) was built to impose off-vertical axis rotation (60 rpm, 45^{o} tilt from the vertical) for 30 minutes as a vestibular stimulus onto mice during motion-sickness testing. The rotator tests two mice at a time, and mice are secured 20 cm from the axis of rotation. When one mouse is tested, an object of equivalent weight is placed into the other cage for balancing before rotation.

Motion-Sickness Index (MSI) Testing**:** As a measurement of motion sickness (MS) in VM, we adapted Yu et al.'s protocol who established this assay to assess the drugs scopolamine and modafinil on mitigating MS in rats and mice (8). We use OVAR as the vestibular challenge (VC).

We utilize the following evaluation criteria for scoring MS in mice at three time points: A) pre-injection/pre-VC, B) post-injection/pre-VC, and C) post-injection/post-VC. Mice were placed in a testing box separate from their home cage to observe for indicators of motion sickness at the specified weights (**Fig. 1A).** Assessment of indicators in A, B, and C occurred in five-minute intervals and were measured in the testing container, whereas indicators from B were determined 20 minutes after injection. Results regarding fecal granules and urination at C include data found

in the testing container and the cages housing mice during the vestibular challenge. A motion sickness index (MSI) score was determined by the summation of the indicators.

Certain actions were taken to normalize the weight distribution of MS indicators during reporting. Of these indicators, only fecal granules (Fg) are counted separately at each time point. We then measured the weight per Fg and back-calculated the excreted feces in grams as an alternative measure to Fg. This calculation was necessary during CGRP testing as mice experienced diarrhea and exact fecal granules would be difficult to count. Thus, in these cases, we measured the mass of excreted feces and made comparisons in terms of mass rather than fecal granule count.

Urination was counted once throughout the experiment's duration and was given a binary weighted scheme (0 for none; 1.2 for seen at either A, B, or C). Piloerection was measured so that the highest individual score is 1.2. If a mouse developed light or severe piloerection at A, B, or C, then 0.6 (light) or 1.2 (severe) was assigned to that timepoint and further timepoints were given a 0. If a mouse suffered light piloerection at A or B, and later developed severe piloerection at B or C respectively, then 0.6 was assigned to the later timepoint so that total summation of piloerection for that animal would be 1.2. Tremors were assigned a score of 1.2 and were noted at any of the three time points in this experiment, with the highest tremor count for an individual mouse set to 3.6.

MSI Experimental Design: In order to reduce the number of injections per mouse, different mice were used to assess the effects of calcitonin gene related peptide (CGRP) or sodium nitroprusside (SNP) on motion sickness indices before and after a vestibular challenge. To reduce the total number of mice tested for motion sickness, animals were repeatedly tested within sub-experiments listed below.

CGRP's effects and CGRP blockade: To test the effects of IP CGRP on motion sickness indices and if olcegepant or sumatriptan can mitigate these changes, 19 mice (9M/10F) were initially allocated to test for vehicle control and 1x CGRP. One male was excluded after CGRP testing due to random death. Mice were later tested with 1x CGRP + 1x olcegepant or 1x CGRP + 1x

sumatriptan. Mice were repeatedly tested to account for intra-animal variability with subsequent tests occurring every 7 days.

SNP's effects: Similarly done with IP CGRP, testing was done to assess systemic SNP's effects on motion sickness indices in a separate group of 18 mice (9M/9F). These mice were tested for vehicle control, 1x SNP, but were not assessed with the drugs olcegepant or sumatriptan.

Drug controls: Mice tested for CGRP blockade were later tested with olcegepant or sumatriptan only as negative controls. Due to the stress induced by repeated injections and repeated testing with OVAR, only nine mice (4M/5F) were tested during sumatriptan only.

Motion-Induced Thermoregulation Testing**:** We adapted Tu et al.'s protocol who first noticed these thermoregulatory changes when measuring the heads, bodies, and tails of mice (7). In this study, head and tail temperatures of C57B6/J mice were measured for a total 45 minutes using a FLIR E60 IR camera (model: E64501). This camera is connected to a tripod and is positioned approximately 43 cm above an open, plexiglass box (mouse box) used to house an individual mouse during testing. Both the tripod and mouse box are securely attached to the surface of the shaker. Briefly, baseline measurements were recorded for five minutes prior to the provocative motion (-5 to 0 mins). The provocative motion was turned ON (75 rpm, 2-cm orbital displacement), and mice were recorded for 20 minutes (0 to 20 mins). The provocative motion was then turned OFF, and mice were recorded for an additional 20 minutes to measure recovery to baseline (20 to 40 mins). Head and tail temperatures were measured after data retrieval using the software FLIR Tools+. Tail and head temperatures were measured within predefined field of views: square region (3x3 mm) for tail and circular region (10x10 mm) for head. Tail measurements occurred 2-3 cm from the base of the tail and head measurements occurred at the center of the head image, in between the mouse's ears. Infrared imaging data was collected every minute during baseline measurements, and every 2 minutes during and after the provocative motion.

We quantified thermoregulatory changes to provocative motion by measuring delta tail vasodilations (^{o}C) and delta head drops (^{o}C). The delta tail vasodilation occurs as a transient increase in the baseline temperature of the tail that quickly returns back to baseline, and so were computed by subtracting the

tail temperature at time t = 0 (rotation ON) from the max tail temperature measured during the first 10 mins of the rotation ($0 \leq t \leq 10$). In order to facilitate quantification and comparisons of the tail vasodilations between treatment groups, a threshold of 1.5^{o}C was imposed upon the data to make it a binary outcome measure. Tail temperature changes equal to or greater than +1.5^{o}C were designated a tail vasodilation and those less than +1.5^{o}C did not meet the criteria. This criterion is used to exclude mice that do not respond to the provocative motion during the vehicle control test, and is also used to assess if mice treated with CGRP+blockers regain tail vasodilations similar to their vehicle test.

For delta heads drops, we subtracted the minimal head temperature during the first 20 minutes of rotation ($0 \leq t \leq 20$) from the head temperature at time t = 0. No thresholds were set on delta head drops.

Motion Induced Thermoregulation Experimental Design: Different mice – not used for motion sickness index (MSI) testing- were used to test CGRP's and SNP's effects on motion-induced nausea. Similar to MSI testing, mice were either tested for CGRP or SNP's effects but not both, and mice were repeatedly tested when addressing the effects of blockers or drug controls to reduce the number of mice used for investigation. Head and tail temperatures were measured before, during, and after a 20-minute provocative motion. Additional experiments were performed to assess test-retest reliability of vehicle control with provocative motion, stationary testing without provocative motion, and provocative motion with varying concentrations of systemically administered CGRP or SNP (listed below).

Stationary Testing: Prior to testing motion-induced thermoregulation, we measured head and tail temperature profiles of mice in the absence of provocative motion for 20 minutes. 18 mice (9M/9F) were used to assess stationary testing after IP injections of either vehicle control, 1x CGRP, or 1x SNP. Repeated testing of these mice occurred 7 days apart.

Test-retest reliability: In order to establish test-retest reliability of the head curves and delta tail vasodilations under vehicle control treatment, 17 mice (9M/8F) were tested. Testing occurred 4-7 days apart. No mice were removed based on the 1.5^{o}C tail vasodilation criteria.

Diluting CGRP's effects (0.1x CGRP and 0.5x CGRP): 19 mice (10M/9F) were used to test the effects of varying IP CGRP concentration on motion-induced thermoregulation. Mice were systemically administered with 0.1x (0.01 mg/kg) and 0.5x (0.05 mg/kg) concentrations of CGRP. Testing occurred 20 minutes after systemic injection. Repeated testing of mice per treatment occurred 7-14 days apart. Of these mice, 12 mice (5M/7F) failed the +1.5^{o}C tail vasodilation criteria when given 0.5x CGRP. These mice were additionally tested 7 days later with a co-administration of 0.5x CGRP + 1x olcegepant to observe for a protective effect of olcegepant at the 0.5x CGRP concentration.

Diluting SNP's effects (0.1x SNP, 0.5x SNP): Similar rationale was used to test the effects of varying IP SNP concentration on motion-induced thermoregulation as was done with IP CGRP. 16 mice (8M/8F) were systemically administered with 0.1x and 0.5x concentrations of SNP prior to testing. Testing occurred 30 minutes after systemic injection, and repeated testing of mice occurred 7 days apart.

CGRP and CGRP+blockers: To test CGRP's effects and if olcegepant or sumatriptan can block these effects, 72 mice (35M/37F) were initially allocated for vehicle control testing. 15 mice (3M/12F) failed the tail vasodilation criterion during vehicle control testing and were excluded from the analysis. An additional 19 mice (12M/7F) were excluded from further testing after vehicle control due to the following reasons: subsequent testing with IP CGRP would occur greater than 14 days after vehicle control testing, mice would be older than 6 months at the time of IP CGRP testing, or death due to random chance. The remaining 38 mice (20M/18F) were then assessed for IP CGRP's effects at the 1x concentration of 0.1 mg/kg. After IP CGRP testing, mice were randomly picked to either receive co-administrations of 1x CGRP + 1x olcegepant or 1x CGRP + 1x sumatriptan but not both; a block randomization protocol was implemented so that mice receiving a particular treatment were housed together (max 5 per cage) to minimize anxiety post treatment. 17 mice (10M/7F) were used to test 1x CGRP + 1x olcegepant, 18 mice (10M/8F) were used to test 1x CGRP + 1x sumatriptan, and the remaining three females were not further tested. We did not exclude animals based on their head temperature profiles. To further assess the effects of triptans, we assessed the effects of 1x CGRP and 1x CGRP + 1x rizatriptan in a different cohort of 14 mice (7M/7F).

SNP and SNP+blockers: As done with IP CGRP, 20 mice (10M/10F) were initially allocated to assess IP SNP's effects and the co-administration of SNP with either olcegepant or sumatriptan. Mice were

assessed at the 1x SNP concentration of 2.5 mg/kg. Four mice (2M/2F) were excluded from the analyses due to failing the +1.5^{o}C tail vasodilation criteria at the vehicle control test. Afterwards, all mice from either sex were repeatedly tested with 1x SNP and then with either 1x SNP + 1x olcegepant or 1x SNP + 1x sumatriptan.

Drug controls: For negative control comparisons, the same mice tested for 1x CGRP + 1x olcegepant (10M/7F) and 1x CGRP + 1x rizatriptan (7M/7F) were later tested with 1x olcegepant only or 1x rizatriptan only respectively. For 1x CGRP + 1x sumatriptan testing, all males but only 6 females were further tested for 1x sumatriptan only.

Power Analyses: G* Power was used to determine study's power. For motion sickness index testing, the number of animals per sex used was predicted to be ten based on power analysis using an alpha of 0.05 with 80% power for repeated-measures M-ANOVA statistical testing (effect size F = 0.79). For motion-induced thermoregulation testing, the number per sex was predicted to be 3 (head temperature) or 4 (tail temperature) based on power analysis using an alpha of 0.05, with 95% power and effect size d=17.33 (based on findings from n=6 mice with nausea-like thermoregulation testing for core body temperature (7). We are overpowered per sex across all motion-induced nausea experiments listed in this study.

Statistical Analyses: Statistical analyses were conducted in GraphPad Prism 9.0. We allocated our motion sickness indices data in the following format. Score patterns for the number of fecal granules (Fg) and the weight of excreted feces (g) were kept separate from other indices. We combined piloerection (P), urination (U), and tremor (T) for a summation score called PUT. Lastly, a final motion-sickness index score (MSI) combining Fg and PUT was computed. These indicators were compared at three different timepoints: pre-injection, post-injection, and post-vestibular challenge. Repeated measures ANOVA is not capable of analyzing data with missing values (i.e., excluded mice), and so a mixed-effects (ME) model approach was the statistical substitute. ME models use a compound symmetry covariance matrix and are fit using Restricted Maximum Likelihood (REML). In the presence of missing values, these results can be interpreted like repeated measures ANOVAs. Sphericity was not assumed during analyses and so a Greenhouse-Geisser correction was applied to results.

When comparing CGRP's effects and CGRP blockade on motion sickness indices (Fg, feces, PUT, MSI), we ran 3-way ME models with the first factor assessing timepoint differences (pre-injection versus post-vestibular challenge, post-injection versus post-vestibular challenge, and pre-injection versus post-injection), the second factor assessing biological sex, and the third factor comparing treatments (CGRP, CGRP+blockers, or SNP). 2-way ME models were run similarly but with biological sex pulled together. Animals used for SNP testing were assessed with 3-way and 2-way repeated measures ANOVAs in an identical organization as 3-way and 2-way ME models used for CGRP testing.

For motion-induced thermoregulation data, two-way ME models were applied to delta tail vasodilations and delta head drops (^{o}C) across the two factors (sex and treatment) for both CGRP and SNP testing. Second-order curve fitting were used to generalize trends in head temperature profiles. Across both assays, Tukey post-hoc comparisons were used to assess for differences between treatment groups compared to vehicle control. For test-retest reliability of head and tail profiles, Pearson's correlation coefficient is listed as r (df), where r is the coefficient and df is the degrees of freedom. Head temperature curves are computed by 2nd order curve fitting and an R^2 value is provided. Values are reported as mean ± SEM unless noted otherwise, and significance was set at $p < 0.05$ for all analyses.

5. Acknowledgements: We would like to acknowledge assistance with data collection and analysis from Vedat Duzgezen, Stefanie Faucher, Elana Fine, Catherine Hauser, Benjamin Liang, and Blaze Strangio. This work was fully supported by NIH R01DC017261.

6. Competing interests: No authors have any financial or non-financial competing interests.

Figure Legends:

Fig. 1: CGRP and SNP's effects on MSI: Female (pink) and male (blue) C57B6J mice were tested for motion sickness indicators. Graphs combining both sexes are depicted in purple. Treatments were delivered intraperitoneally (IP): vehicle control (open circle/open square), CGRP (closed circle), SNP (closed square), olcegepant + CGRP (top half-filled circle), and sumatriptan + CGRP (bottom half-filled circle). **(A)** Assay timeline is illustrated and a table of criteria and scoring is provided. Motion sickness index (MSI) was computed by a summation of criterion at the appropriate scoring and involved measuring feces, piloerection, urination, and tremor. MSI was recorded at three different time points: pre-injection, post-injection, and post-vestibular challenge. The vestibular challenge involved off-vertical axis rotation (60 rpm, 45^{o} tilt from the vertical) for 30 minutes. **(B-D)** In animals allocated for assessing CGRP's effects, MSI outcomes significantly increased after injection and after the vestibular challenge for all treatments**.** Tukey post-hoc indicated increased MSI after IP CGRP (adj. $p < 0.0001$) or after IP CGRP+sumatriptan (adj. $p = 0.0002$) compared to vehicle control. **(E-G)** When testing SNP's effects, significant differences were seen in MSI outcomes after injection and after the challenge, but no differences were seen when comparing vehicle control versus SNP.

Fig. 2: Fecal excretion exaggerates MSI outcome: Feces weight (grams) was measured by back-calculating the weight per fecal granule and multiplying by the number of granules measured. **(A-C)** When assessing CGRP and CGRP+blockers, significant differences in collected feces were observed after injection and after the vestibular challenge. Tukey post-hoc analysis showed increased fecal excretion after CGRP (adj. $p < 0.0001$) and after CGRP+sumatriptan (adj. $p = 0.0001$) similar to MSI values. **(D-F)** Mice assessed for SNP's effects showed increased fecal excretion after each time point, but no differences were seen compared to vehicle control.

Fig. 3: PUT outcome does not differ between treatments: PUT was computed by summing normalized piloerection, urination, and tremor. PUT outcome increased after injection and after the vestibular challenge, but no differences were observed between treatments for **(A-C)** CGRP testing or **(D-F)** SNP testing.

Fig. 4: Stationary and provocative motion testing after IP vehicle control: (A) Using a FLIR E60 infrared camera, head and tail temperatures for all conditions are recorded before, during, and after a provocative twenty-minute orbital rotation acting as the vestibular challenge. Infrared recordings are 45 minutes in duration. (**B-E**). Sample sizes are depicted in the bottom left for female (pink) and male (blue) C57B6/J mice. After administering vehicle control (saline), **(B and C)** head and **(D and E)** tail temperatures were compared during **(C and E)** stationary testing or **(B and D)** during the provocative rotation**.** Head temperatures for stationery and VC testing were fit to the second-order curve (B_2X^2 + B_1X + B_0) and delta head temperatures were computed by subtracting temperature at time t = 20 mins from t = 0 mins. Head curves compute a delta head difference of -1.22^{o}C for females and -1.62^{o}C for males during VC testing and a difference of 0.70^{o}C for females and 0.27^{o}C for males during stationary testing. Delta tail vasodilations were computed by averaging individual tail responses and are depicted as group averages +/- standard error of the mean (SEM). During the first 10 minutes of the provocative rotation, delta tail vasodilations were computed to be 4.6 ±0.3^{o}C for females and 6.1 ± 0.4^{o}C for males. Mice during stationary testing did not experience delta tail vasodilations, and thus a similar computation led to delta tail changes of -1.1 ± 0.8^{o}C for females and 0.2 ± 0.6^{o}C for males.

Fig. 5: Stationary testing after IP CGRP/SNP and test-retest of IP vehicle control. Sample sizes are listed in the upper left corner. **(A and B)** Head temperature curves were recorded during stationary testing after IP delivery of vehicle control, 1x CGRP, and 1x SNP. **(C and F)** A different cohort of mice was used to assess the test-retest reliability of head and tail temperatures during provocative rotation. **(C)** When assessing test-retest reliability, no significant differences were seen in the mean magnitude of delta head drops in females (test vs retest: -1.2 ^{o}C vs -1.2 ^{o}C) or males (test vs retest: -1.3 vs 1.2 ^{o}C). (**D and E**) Tail temperatures were compared between stationary tests for IP vehicle, IP CGRP, and IP SNP as similarly done with head temperatures, and no significant differences were seen. **(F)** Similar to head temperatures, test-retest of tail measurements during provocative rotation showed no significant differences in delta tail vasodilations in either female (test vs retest: 4.0 ± 0.8 ^{o}C vs 4.2 ± 0.8 ^{o}C) or male (test vs retest: 4.9 ± 0.8 ^{o}C vs 4.9 ± 0.9 ^{o}C).

Fig. 6: CGRP/SNP effects on hypothermia to provocative motion and dose-dependent changes in tail vasodilations. Sample sizes are shown in the upper right corner. Mice allocated for assessing CGRP's effects on head and tail temperatures were tested for **(A and E)** vehicle control and then **(B and F)** 1x CGRP at 0.1 mg/kg. When assessing head temperature recovery, the 2nd-order curve fits extrapolated recovery times for vehicle control (female: 20.3 mins, male: 20.4 mins) and IP CGRP (females: 28.4 mins, male: 25.4 mins). Delta tail vasodilations were observed under vehicle control (female: 4.56 ± 0.31 ^{o}C, male: 6.05 ± 0.35 ^{o}C) but were significantly diminished after 1x IP CGRP delivery (female: 0.61 ± 0.20 ^{o}C, male: 1.92 ± 0.40 ^{o}C). A separate mice cohort was allocated for assessing SNP's effects on head and tail and was tested for **(C and G)** vehicle control and later **(D and H)** 1x SNP at 2.5 mg/kg. While head temperature recovery did not differ between vehicle and 1x IP SNP groups, delta tail vasodilations were diminished after 1x IP SNP delivery (female: 0.3 ± 0.1 ^{o}C, male: 1.1 ± 0.5 ^{o}C) when compared to vehicle control (female: 4.2 ± 1.0 ^{o}C, male: 3.4 ± 0.5 ^{o}C). **(I – L)** Dose-dependent changes in tail temperatures were observed for both IP CGRP and IP SNP. For CGRP testing, 0.1x, 0.5x, and 1x concentrations were prepared at 0.01, 0.05, and 0.1 mg/kg. For SNP testing, 0.1x, 0.5x, and 1x concentrations were prepared at 0.25 mg/kg, 1.25, and 2.5 mg/kg.

Fig. 7: Olcegepant, but not sumatriptan or rizatriptan, protects against CGRP's effects on tail vasodilations: (A-H) Sample sizes are labeled in the bottom right corner. Tail temperatures were recorded IP delivery of vehicle control, CGRP, CGRP+olcegepant, and CGRP + sumatriptan. Before-after plots show changes in delta tail vasodilations in repeatedly tested male and female mice after **(I)** 1x CGRP and 1x CGRP + olcegepant or after **(J)** 1x CGRP and 1x CGRP + sumatriptan. When compared to vehicle control, Tukey post-hoc analysis showed delta tail vasodilations were significantly diminished after CGRP (adj. $p < 0.0001$) and after CGRP+sumatriptan (adj. $p<0.001$) delivery in either sex but no significant differences with CGRP+olcegepant. Mice treated with 0.5x IP CGRP and experienced reduced delta tail vasodilations compared to vehicle control regained near normal vasodilations when treated with IP 0.5x CGRP + olcegepant. **(L)** The effects of CGRP+rizatriptan were observed in a different cohort of mice (n = 7M/7F) and delta tail vasodilations were significantly

diminished after IP CGRP (females, adj. p = 0.02; males adj. p = 0.001) and were still diminished after IP CGRP + rizatriptan (females, adj. p = 0.01; males, adj. p = 0.003) compared to vehicle control. **(M)** A floating bar plot is used to compare all animals used to assess CGRP and CGRP+blockers' effects on delta tail vasodilations.

Fig. 8: Olcegepant and sumatriptan block SNP's effects on tail vasodilations: (A-H) Similar to CGRP testing, tail temperatures were recorded after IP delivery of vehicle control, SNP, SNP+olcegepant, and SNP+sumatriptan, and sample sizes are labeled in the bottom right corner. Before-after plots show changes in delta tail vasodilations in mice after **(I)** 1x SNP and 1x SNP + olcegepant or after **(J)** 1x SNP and 1x SNP + sumatriptan. Tukey's post-hoc analysis showed that SNP diminished delta tail vasodilations compared to vehicle control in both sexes (female, adj. p = 0.015; male, adj. p = 0.0002), but saw no difference between vehicle vs IP SNP+olcegepant or vehicle vs IP SNP+sumatriptan. **(K)** A floating bar graph depicts delta tail values for all mice assessed with SNP or SNP+blockers.

Table Legends:

Table 1: Three-way mixed effects models were computed to assess the effects of time of criteria measurement (pre-injection, post-injection, post-vestibular challenge (VC)) and treatment (CGRP, CGRP+blockers, or SNP) . Male and female mice were grouped together. Separate groups of mice were used to compare effects of CGRP/CGRP+Blockers or SNP. The Geisser-Greenhouse Correction (ε̂) was applied due to time of observations and treatment being repeated measures. Tukey post-hoc comparisons wee made for each treatment between the time period T1 versus time period T2, where A = pre-injection, AB = post-injection, and ABC = post-vestibular challenge. Mice were repeatedly tested and corresponds to a sample size N. Mean differences are computed by T2 - T1, where MSI has arbitrary units, and feces unites are in unit grams based on calculating mass of counted fecal granules. For tabular results and multiple comparisons, F and P-values are listed accordingly.

Table 2: Two-way mixed-effects models were computed to assess the effects of treatment (CGRP, SNP, or CGRP/SNP + Blockers) on delta tail vasodilations. Mice were separated by sex and the interaction of treatment x sex was also considered. Separate groups of mice were used to compare the effects of CGRP/CGRP+Blockers or SNP/SNP+Blockers. The Geisser-Greenhouse Correction ($\hat{\varepsilon}$) was applied to factors that are repeated measures. Tukey post-hoc comparisons are described in relation to vehicle control in males and females. For tabular results and multiple comparisons, F and P-values are listed accordingly.

Table 3: Diminished tail vasodilations indicate a disrupted response to provocative rotation. Percentage of mice that exhibited diminished delta tail vasodilations (<1.5^{o} C) during motion-induced thermoregulation testing across treatment. Treatments are administered at the following concentrations: 0.1x CGRP - 0.01 mg/kg, 0.5x CGRP - 0.05 mg/kg, 1x CGRP - 0.1 mg/kg, 1x olcegepant - 1 mg/kg, sumatriptan - 0.6 mg/kg, rizatriptan - 0.6 mg/kg, SNP - 2.5 mg/kg.

7. References:

1. Ozcelik P, Kocoglu K, Ozturk V, Keskinoglu P, Akdal G. Characteristic differences between vestibular migraine and migraine only patients. J Neurol. 2022;269(1):336-41. Epub 2021/06/11. doi: 10.1007/s00415-021-10636-0. PubMed PMID: 34109480.

2. Wang J, Lewis RF. Contribution of intravestibular sensory conflict to motion sickness and dizziness in migraine disorders. J Neurophysiol. 2016;116(4):1586-91. Epub 2016/07/08. doi: 10.1152/jn.00345.2016. PubMed PMID: 27385797; PMCID: PMC5144688.

3. Wurthmann S, Naegel S, Roesner M, Nsaka M, Scheffler A, Kleinschnitz C, Holle D, Obermann M. Sensitized rotatory motion perception and increased susceptibility to motion sickness in vestibular migraine: A cross-sectional study. Eur J Neurol. 2021;28(7):2357-66. Epub 2021/04/30. doi: 10.1111/ene.14889. PubMed PMID: 33914990.

4. Wang J, Lewis RF. Abnormal Tilt Perception During Centrifugation in Patients with Vestibular Migraine. J Assoc Res Otolaryngol. 2016;17(3):253-8. Epub 2016/03/10. doi: 10.1007/s10162-016-0559-7. PubMed PMID: 26956976; PMCID: PMC4854827.

5. Cha YH, Golding JF, Keshavarz B, Furman J, Kim JS, Lopez-Escamez JA, Magnusson M, Yates BJ, Lawson BD, Advisors. Motion sickness diagnostic criteria: Consensus Document of the Classification Committee of the Barany Society. J Vestib Res. 2021;31(5):327-44. Epub 2021/03/02. doi: 10.3233/VES-200005. PubMed PMID: 33646187.

6. Nalivaiko E, Rudd JA, So RH. Motion sickness, nausea and thermoregulation: The "toxic" hypothesis. Temperature (Austin). 2014;1(3):164-71. Epub 2014/10/01. doi: 10.4161/23328940.2014.982047. PubMed PMID: 27626043; PMCID: PMC5008705.

7. Tu L, Poppi L, Rudd J, Cresswell ET, Smith DW, Brichta A, Nalivaiko E. Alpha-9 nicotinic acetylcholine receptors mediate hypothermic responses elicited by provocative motion in mice. Physiol Behav. 2017;174:114-9. doi: 10.1016/j.physbeh.2017.03.012. PubMed PMID: 28302571.

8. Yu XH, Cai GJ, Liu AJ, Chu ZX, Su DF. A novel animal model for motion sickness and its first application in rodents. Physiol Behav. 2007;92(4):702-7. doi: 10.1016/j.physbeh.2007.05.067. PubMed PMID: 17612582.

9. Wei X, Wang ZB, Zhang LC, Liu WY, Su DF, Li L. Verification of motion sickness index in mice. CNS Neurosci Ther. 2011;17(6):790-2. Epub 2011/11/29. doi: 10.1111/j.1755-5949.2011.00272.x. PubMed PMID: 22117804; PMCID: PMC6493908.

10. Ashina H, Newman L, Ashina S. Calcitonin gene-related peptide antagonism and cluster headache: an emerging new treatment. Neurol Sci. 2017. doi: 10.1007/s10072-017-3101-8. PubMed PMID: 28856479.

11. Edvinsson L. CGRP blockers in migraine therapy: where do they act? Br J Pharmacol. 2008;155(7):967-9. Epub 2008/09/09. doi: bjp2008346 [pii]

10.1038/bjp.2008.346. PubMed PMID: 18776915; PMCID: 2597260.

12. Edvinsson L. The Trigeminovascular Pathway: Role of CGRP and CGRP Receptors in Migraine. Headache. 2017;57 Suppl 2:47-55. doi: 10.1111/head.13081. PubMed PMID: 28485848.

13. Russo AF. CGRP as a neuropeptide in migraine: lessons from mice. Br J Clin Pharmacol. 2015;80(3):403-14. doi: 10.1111/bcp.12686. PubMed PMID: 26032833; PMCID: PMC4574826.

14. Russo AF. Calcitonin gene-related peptide (CGRP): a new target for migraine. Annu Rev Pharmacol Toxicol. 2015;55:533-52. doi: 10.1146/annurev-pharmtox-010814-124701. PubMed PMID: 25340934; PMCID: 4392770.

15. Goadsby PJ, Lipton RB, Ferrari MD. Migraine--current understanding and treatment. N Engl J Med. 2002;346(4):257-70. doi: 10.1056/NEJMra010917. PubMed PMID: 11807151.

16. Lassen LH, Haderslev PA, Jacobsen VB, Iversen HK, Sperling B, Olesen J. CGRP may play a causative role in migraine. Cephalalgia. 2002;22(1):54-61. PubMed PMID: 11993614.

17. Tringali G, Navarra P. Anti-CGRP and anti-CGRP receptor monoclonal antibodies as antimigraine agents. Potential differences in safety profile postulated on a pathophysiological basis. Peptides. 2019;116:16-21. Epub 2019/04/25. doi: 10.1016/j.peptides.2019.04.012. PubMed PMID: 31018157.

18. Scuteri D, Adornetto A, Rombola L, Naturale MD, Morrone LA, Bagetta G, Tonin P, Corasaniti MT. New Trends in Migraine Pharmacology: Targeting Calcitonin Gene-Related Peptide (CGRP) With Monoclonal Antibodies. Front Pharmacol. 2019;10:363. Epub 2019/04/27. doi: 10.3389/fphar.2019.00363. PubMed PMID: 31024319; PMCID: PMC6465320.

19. Bates EA, Nikai T, Brennan KC, Fu YH, Charles AC, Basbaum AI, Ptacek LJ, Ahn AH. Sumatriptan alleviates nitroglycerin-induced mechanical and thermal allodynia in mice. Cephalalgia. 2010;30(2):170-8. Epub 2009/06/06. doi: 10.1111/j.1468-2982.2009.01864.x. PubMed PMID: 19489890; PMCID: PMC4854191.

20. Recober A, Kuburas A, Zhang Z, Wemmie JA, Anderson MG, Russo AF. Role of calcitonin gene-related peptide in light-aversive behavior: implications for migraine. J Neurosci. 2009;29(27):8798-804. doi: 10.1523/JNEUROSCI.1727-09.2009. PubMed PMID: 19587287; PMCID: 2944225.

21. Wang M, Duong TL, Rea BJ, Waite JS, Huebner MW, Flinn HC, Russo AF, Sowers LP. CGRP Administration Into the Cerebellum Evokes Light Aversion, Tactile Hypersensitivity, and Nociceptive Squint in Mice. Front Pain Res (Lausanne). 2022;3:861598. Epub 2022/05/14. doi: 10.3389/fpain.2022.861598. PubMed PMID: 35547239; PMCID: PMC9082264.

22. Falkenberg K, Bjerg HR, Olesen J. Two-Hour CGRP Infusion Causes Gastrointestinal Hyperactivity: Possible Relevance for CGRP Antibody Treatment. Headache: The Journal of Head and Face Pain. 2020;60(5):929-37. doi: 10.1111/head.13795.

23. Chan TLH, Cowan RP, Woldeamanuel YW. Calcitonin Gene-Related Peptide Receptor Antagonists (Gepants) for the Acute Treatment of Nausea in Episodic Migraine: A Systematic Review and Meta-Analysis. Headache. 2020;60(7):1489-99. Epub 2020/06/10. doi: 10.1111/head.13858. PubMed PMID: 32515018.

24. Araya EI, Turnes JM, Barroso AR, Chichorro JG. Contribution of intraganglionic CGRP to migraine-like responses in male and female rats. Cephalalgia. 2020;40(7):689-700. Epub 2019/12/21. doi: 10.1177/0333102419896539. PubMed PMID: 31856582.

25. Mason BN, Kaiser EA, Kuburas A, Loomis MM, Latham JA, Garcia-Martinez LF, Russo AF. Induction of Migraine-Like Photophobic Behavior in Mice by Both Peripheral and Central CGRP Mechanisms. J Neurosci. 2017;37(1):204-16. doi: 10.1523/JNEUROSCI.2967-16.2017. PubMed PMID: 28053042; PMCID: PMC5214631.

26. Rea BJ, Wattiez AS, Waite JS, Castonguay WC, Schmidt CM, Fairbanks AM, Robertson BR, Brown CJ, Mason BN, Moldovan-Loomis MC, Garcia-Martinez LF, Poolman P, Ledolter J, Kardon RH,

Sowers LP, Russo AF. Peripherally administered calcitonin gene-related peptide induces spontaneous pain in mice: implications for migraine. Pain. 2018;159(11):2306-17. Epub 2018/07/12. doi: 10.1097/j.pain.0000000000001337. PubMed PMID: 29994995; PMCID: PMC6193822.

27. Kaiser EA, Rea BJ, Kuburas A, Kovacevich BR, Garcia-Martinez LF, Recober A, Russo AF. Anti-CGRP antibodies block CGRP-induced diarrhea in mice. Neuropeptides. 2017;64:95-9. Epub 2016/11/21. doi: 10.1016/j.npep.2016.11.004. PubMed PMID: 27865545; PMCID: PMC5429995.

28. Holzer P, Holzer-Petsche U. Constipation Caused by Anti-calcitonin Gene-Related Peptide Migraine Therapeutics Explained by Antagonism of Calcitonin Gene-Related Peptide's Motor-Stimulating and Prosecretory Function in the Intestine. Front Physiol. 2021;12:820006. Epub 2022/01/29. doi: 10.3389/fphys.2021.820006. PubMed PMID: 35087426; PMCID: PMC8787053.

29. Allais G, Chiarle G, Sinigaglia S, Airola G, Schiapparelli P, Benedetto C. Gender-related differences in migraine. Neurol Sci. 2020;41(Suppl 2):429-36. Epub 2020/08/28. doi: 10.1007/s10072-020-04643-8. PubMed PMID: 32845494; PMCID: PMC7704513.

30. Huang TC, Wang SJ, Kheradmand A. Vestibular migraine: An update on current understanding and future directions. Cephalalgia. 2020;40(1):107-21. Epub 2019/08/10. doi: 10.1177/0333102419869317. PubMed PMID: 31394919.

31. Shen Y, Qi X, Wan T. The Treatment of Vestibular Migraine: A Narrative Review. Ann Indian Acad Neurol. 2020;23(5):602-7. Epub 2021/02/25. doi: 10.4103/aian.AIAN_591_19. PubMed PMID: 33623258; PMCID: PMC7887465.

32. Avona A, Burgos-Vega C, Burton MD, Akopian AN, Price TJ, Dussor G. Dural Calcitonin Gene-Related Peptide Produces Female-Specific Responses in Rodent Migraine Models. The Journal of Neuroscience. 2019;39(22):4323-31. doi: 10.1523/jneurosci.0364-19.2019.

33. Paige C, Plasencia-Fernandez I, Kume M, Papalampropoulou-Tsiridou M, Lorenzo L-E, David ET, He L, Mejia GL, Driskill C, Ferrini F, Feldhaus AL, Garcia-Martinez LF, Akopian AN, De Koninck Y, Dussor G, Price TJ. A Female-Specific Role for Calcitonin Gene-Related Peptide (CGRP) in Rodent Pain Models. The Journal of Neuroscience. 2022;42(10):1930-44. doi: 10.1523/jneurosci.1137-21.2022.

34. Ji Y, Rizk A, Voulalas P, Aljohani H, Akerman S, Dussor G, Keller A, Masri R. Sex differences in the expression of calcitonin gene-related peptide receptor components in the spinal trigeminal nucleus.

Neurobiol Pain. 2019;6:100031. Epub 2019/06/22. doi: 10.1016/j.ynpai.2019.100031. PubMed PMID: 31223141; PMCID: PMC6565752.

35. Akerman S, Karsan N, Bose P, Hoffmann JR, Holland PR, Romero-Reyes M, Goadsby PJ. Nitroglycerine triggers triptan-responsive cranial allodynia and trigeminal neuronal hypersensitivity. Brain. 2019;142(1):103-19. Epub 2019/01/01. doi: 10.1093/brain/awy313. PubMed PMID: 30596910; PMCID: PMC6308314.

36. Ernstsen C, Christensen SL, Olesen J, Kristensen DM. No additive effect of combining sumatriptan and olcegepant in the GTN mouse model of migraine. Cephalalgia. 2021;41(3):329-39. Epub 2020/10/17. doi: 10.1177/0333102420963857. PubMed PMID: 33059476.

37. Tvedskov JF, Tfelt-Hansen P, Petersen KA, Jensen LT, Olesen J. CGRP receptor antagonist olcegepant (BIBN4096BS) does not prevent glyceryl trinitrate-induced migraine. Cephalalgia. 2010;30(11):1346-53. Epub 2010/10/21. doi: 10.1177/0333102410363491. PubMed PMID: 20959429.

38. Zhong W, Shahbaz O, Teskey G, Beever A, Kachour N, Venketaraman V, Darmani NA. Mechanisms of Nausea and Vomiting: Current Knowledge and Recent Advances in Intracellular Emetic Signaling Systems. Int J Mol Sci. 2021;22(11). Epub 2021/06/03. doi: 10.3390/ijms22115797. PubMed PMID: 34071460; PMCID: PMC8198651.

39. Holland PR, Saengjaroentham C, Vila-Pueyo M. The role of the brainstem in migraine: Potential brainstem effects of CGRP and CGRP receptor activation in animal models. Cephalalgia. 2019;39(3):390-402. Epub 2018/02/08. doi: 10.1177/0333102418756863. PubMed PMID: 29411638.

40. Lessem SE. QuickStats: Percentage of Adults Who Had a Severe Headache or Migraine in the Past 3 months, by Sex and Age Grou - National Health Interview Survey, United States, 2018. In: Statistics NCfH, editor. Morbidity and Mortality Weekly Report (MMWR). March 27th, 2020 ed2018.

41. Meyer CW, Ootsuka Y, Romanovsky AA. Body Temperature Measurements for Metabolic Phenotyping in Mice. Front Physiol. 2017;8:520. Epub 2017/08/22. doi: 10.3389/fphys.2017.00520. PubMed PMID: 28824441; PMCID: PMC5534453.

42. Furman JM, Schor RH, Schumann TL. Off-vertical axis rotation: a test of the otolith-ocular reflex. Ann Otol Rhinol Laryngol. 1992;101(8):643-50. Epub 1992/08/01. doi: 10.1177/000348949210100803. PubMed PMID: 1497268.

43. Hess BJM, Dieringer N. Spatial Organization of the Maculo-Ocular Reflex of the Rat: Responses During Off-Vertical Axis Rotation. European Journal of Neuroscience. 1990;2(11):909-19. doi: 10.1111/j.1460-9568.1990.tb00003.x.

44. Beraneck M, Bojados M, Le Seac'h A, Jamon M, Vidal PP. Ontogeny of mouse vestibulo-ocular reflex following genetic or environmental alteration of gravity sensing. PLoS One. 2012;7(7):e40414. Epub 2012/07/19. doi: 10.1371/journal.pone.0040414. PubMed PMID: 22808156; PMCID: PMC3393735.

45. Dai M, Sofroniou S, Kunin M, Raphan T, Cohen B. Motion sickness induced by off-vertical axis rotation (OVAR). Exp Brain Res. 2010;204(2):207-22. Epub 2010/06/11. doi: 10.1007/s00221-010-2305-4. PubMed PMID: 20535456; PMCID: PMC3181161.

46. Dai M, Kunin M, Raphan T, Cohen B. The relation of motion sickness to the spatial-temporal properties of velocity storage. Exp Brain Res. 2003;151(2):173-89. Epub 2003/06/05. doi: 10.1007/s00221-003-1479-4. PubMed PMID: 12783152.

47. Idoux E, Tagliabue M, Beraneck M. No Gain No Pain: Relations Between Vestibulo-Ocular Reflexes and Motion Sickness in Mice. Front Neurol. 2018;9:918. Epub 2018/11/30. doi: 10.3389/fneur.2018.00918. PubMed PMID: 30483206; PMCID: PMC6240678.